Available online at www.sciencedirect.com
ScienceDirect
Food Hydrocolloids 21 (2007) 100–109
FOOD HYDROCOLLOIDS
www.elsevier.com/locate/foodhyd

Effect of pH and ionic strength on apple juice turbidity: Application of the extended DLVO theory

Elisa I. Benítez, Diego B. Genovese*, Jorge E. Lozano

PLAPIQUI (UNS-CONICET), Camino La Carrindanga Km 7, 8000 Bahía Blanca, Argentina

Received 12 December 2005; accepted 24 February 2006

Abstract

This work studied the effect of liquid medium pH and ionic strength on the stability of apple juice particles. Colloidal interactions between them were modeled with the extended DLVO theory. Considering that repulsive forces provide sol stability, its turbidity was modeled to be the sum of a "hydration contribution" plus an "electrostatic contribution". Sol turbidity followed a linear relationship with the energy barrier between pairs of particles, which prevents their agglomeration (energy barrier information was obtained from viscosity—particle volume fraction data). The turbidity predicted for zero energy barrier was significantly high, indicating that particles were inherently stable. This was attributed to an immobilized water layer coating them (the primary hydration shell). Energy barrier was governed by changes in particles surface charge (ζ potential) and hydration constant: they decreased at decreasing pH and increasing ionic strength. ζ potential's reduction was attributed to neutralization of particles negative charge, and compression of the electrical double layer surrounding them, respectively. Hydration's decrease was attributed to the distortion of the outer hydration shells by hydrated cations attracted by particles negative charge.

Keywords: Apple juice; Turbidity; DLVO theory; Stability; pH; Ionic strength

1. Introduction

Natural fruit juices are complex multicomponent systems, opalescent or turbid due to the presence of insoluble solids in suspension. These solids are mainly composed of carbohydrates and proteins, which are insoluble at the juice pH (Dietrich, Gierschner, Pecoroni, Zimmer, & Will, 1996). The proteins have acid and basic groups whose degree of ionization depends on the pH and ionic strength of the liquid medium (Magdassi & Kamyshny, 1996). Fruit juice particles have been suggested to be covered by a protective pectin layer, negatively charged at the juice pH (Sorrivas, Genovese, & Lozano, 2006; Yamasaki, Yasui, & Arima, 1964). The pectin present both in solution and coating of the particles prevents the contact between them, providing stability to the juice. To elaborate clarified juices the native pectin must be degraded and removed since it complicates the clarification process. After juice depectinization, only negatively charged colloidal particles smaller than 0.5 μm remain in suspension, since bigger particulate material precipitates by gravity (Beveridge, 2002). This system may be then considered to be a solid–liquid colloidal dispersion (sol). Particles negative charge is attributed to degraded pectin molecules that remain bonded to the surface.

Since particle volume fraction in cloudy apple juices is smaller than 0.5% (Genovese & Lozano, 2000) it may be considered that only interaction between pairs of particles takes place (Overbeek, 1977). Then, the classic DLVO theory developed by Derjaguin, Landau, Verwey and Overbeek (Derjaguin, 1989; Overbeek, 1977) would be valid to explain the tendency of these colloids to agglomerate or remain free. This theory combines the Van der Waals attraction forces and the electrostatic repulsion forces as a function of the distance between pairs of particles: the combined curve is called the net interaction energy. The point of maximum repulsive energy is known as the energy barrier. To agglomerate two encountering particles, they must have enough kinetic energy (due to

*Corresponding author. Tel.: +54 291 486 1700; fax: +54 291 486 1600.
E-mail address: dgenovese@plapiqui.edu.ar (D.B. Genovese).

0268-005X/$ - see front matter © 2006 Elsevier Ltd. All rights reserved.
doi:10.1016/j.foodhyd.2006.02.007

their speed and mass) to overcome that barrier. Then, the flocculation degree will depend on the particles collision frequency and their energy respect to the energy barrier (Sennet & Olivier, 1965). Boström, Williams, and Ninham (2001) indicated that traditional DLVO theory works well for low salts concentration, on the order of 0.01 M. Although this theory has been widely used, it does not explain correctly the behavior of hydrophilic colloidal particles in aqueous medium since they can form hydrogen bonds with water, or else attract hydrated ions generating the so-called hydration forces (McClements, 1999).

It has been reported (Genovese & Lozano, 2006a) that reducing the pH of cloudy apple juice reduced the particles surface charge (ζ potential), but particles were not destabilized because turbidity was not significantly affected. Consequently, it became evident that the two forces involved in the classic DLVO theory are not enough to explain the colloidal stability of these juices, and therefore the hydration force has to be considered. It has been proposed (Genovese & Lozano, 2006a, 2006b) that apple juice particles have dipolar or ionic groups that may be hydrated (e.g., –OH, $–COO^-$, NH_3^+), and some may also be capable of binding hydrated ions (e.g., $-COO^- + K^+ \rightarrow -COO^-K^+$). It seems that the polysaccharides (mainly galactose and arabinose) coming from pectin degradation and also integrating the colloidal particles (Brillouet, Williams, Will, Müller, & Pellerin, 1996) form hydrogen bonds with water molecules, hydrating the particles and giving them high stability. D-galacturonic acid residues occur in pectins and tightly bind some water molecules. However, the amount bound strongly depends mostly on the cation counterion present rather than the sugar residue (Zavitsas, 2001).

The objectives of this work were: (a) to determine the effect of both pH and ionic strength on apple juice particles stability; (b) to predict the individual contribution of repulsive (electrostatic and hydration) forces to sol turbidity; (c) to estimate the energy barrier between pairs of particles; (d) to correlate turbidity and energy barrier; and (e) to estimate the hydration constant.

2. Theory

2.1. Extended DLVO theory

The Van der Waals attractive energy (U_A) between spherical particles of radius a can be expressed as (Overbeek, 1977):

$$U_A(x) = -\frac{A}{6}\left[\left(\frac{2a^2}{x^2+4ax}\right)+\frac{2a^2}{x^2+4ax+4a^2} + \ln\left(\frac{x^2+4ax}{x^2+4ax+4a^2}\right)\right], \quad (1)$$

where x is the separation distance between the surfaces of the spheres, and A is the Hamaker constant, whose value depends on the properties of the particles and the dispersing medium. At close separations ($x \ll a$) the above equation may be simplified considerably (McClements, 1999):

$$U_A(x) = -\frac{aA}{12x}. \quad (2)$$

For small particle's surface potentials (ψ_0) and $\kappa a > 10$, the electrostatic repulsive energy (U_E) is given by the expression (Quemada & Berli, 2002):

$$U_E(x) = 2\pi\varepsilon a\psi_0^2 \ln[1+\exp(-\kappa x)], \quad (3)$$

where ε is the permittivity of the medium, and κ^{-1} is the thickness of the electrical double layer surrounding the particle, or Debye's length:

$$\kappa^{-1} = \sqrt{\frac{\varepsilon k_B T}{2IeF}}, \quad (4)$$

where k_B is the Boltzmann constant, T is the temperature, e is the electronic charge, F is Faraday's constant, and I is the ionic strength calculated as

$$I = \frac{1}{2}\sum c_i z_i^2, \quad (5)$$

where z_i and c_i are the valence and molar concentration of ions i in the bulk, respectively (Overbeek, 1977).

Hydration interactions arise from the structuring of water molecules around dipolar and ionic groups. As two particles approach each other, the bonds between the polar groups and the water molecules in the immediate vicinity must be disrupted, which results in a repulsive interaction (Besseling, 1997). The greater the degree of hydration, the more repulsive and long range the interaction (Israelachvili, 1992). It is difficult to develop theories from first principles to describe this type of interaction because of the complex nature of its origin and its dependence on the specific type of ions and polar groups present (McClements, 1999).

Generally, for a solvated surface, solvent molecules highly restricted in their motion experience structural forces. When the solvent is water, this orientation restriction is referred to as hydration pressure (Israelachvili, 1992). This effect is not limited to a primary hydration shell, but rather it propagates radially towards the bulk solution in to a secondary hydration shell. In this second hydration shell, the hydration pressure still exists, but there is less restriction to the rotation of water molecules (Grasso, Subramaniam, Butkus, Strevett, & Bergendahl, 2002). As hydration pressure decays exponentially with distance, an empirical function has been developed for the hydration energy (U_H):

$$U_H(x) = aP_0\lambda\exp(-x/\lambda), \quad (6)$$

where P_0 is the hydration pressure constant which depends on the degree of hydration of the surface (typically between 3 and 30 mJ/m^{-2}), and λ is the characteristic decay length of the interaction (typically between 0.6 and 1.1 nm) (Israelachvili, 1992).

The hydration energy has been included in the extended DLVO theory, such that the total interaction energy (U_T) between pairs of particles is

$$U_T(x) = U_A(x) + U_E(x) + U_H(x). \quad (7)$$

Given the proper values to the parameters involved in Eqs. (2), (3) and (6), the total energy curve can be represented as a function of interparticle distance. Since the energy barrier (U_{Max}) is the primary maximum of the energy curve, it can be obtained at the point where the derivative of Eq. (7) with respect to x equals zero:

$$\left.\frac{dU_T}{dx}\right|_X = \frac{-2\pi\varepsilon a\psi_0^2\kappa\exp(-\kappa X)}{1+\exp(-\kappa X)} + \frac{aA}{12X^2} - aP_0\exp(-X/\lambda) = 0 \quad (8)$$

being X the interparticle distance where the energy barrier is located, such that: $U_T(X) = U_{Max}$. In this study, the energy barrier was modified by changing the pH and I, since these factors affect directly the forces involved.

When the U_T vs. x diagram presents no energy barrier, agglomeration is expected to occur spontaneously and the turbidity will reach a minimum. As the electrostatic interaction energy increases, e.g., by increasing pH above the isoelectric point (pI) or by decreasing the ionic strength, the energy barrier increases, stabilizing the suspension and, hence, increasing the turbidity (Chang & Chang, 2002; Yotsumoto & Yoon, 1993a). Thus, for a colloidal suspension with given particles' size and refractive index, turbidity is uniquely defined by the energy barrier. On this base, an empirical correlation between turbidity and energy barrier was proposed in this work. Combining this correlation with the viscosity model proposed by Genovese and Lozano (2006b) for diluted colloidal dispersions (Eq. (12)), and the extended DLVO theory (Eqs. (7) and (8)), estimated values of the energy barrier and the hydration constant can be obtained for different conditions of the liquid medium.

2.2. Viscosity model

The viscosity of a colloidal suspension (η) has been modeled (Berli, Deiber, & Añón, 1999; Ogawa, Yamada, Matsuda, & Okajima, 1997; Quemada & Berli, 2002) as the sum of a "hard-sphere" contribution (η^{hs}) and a "colloidal forces" contribution (η^{cf}):

$$\eta = \eta^{hs} + \eta^{cf}. \quad (9)$$

The term η^{hs} is considered to be the viscosity of an ideal suspension of rigid, non-interacting (inert), spherical particles. In the dilute regime, the well-known Einstein's equation (Eq. (10)) predicts it in terms of the volume fraction of particles (ϕ), and the viscosity of the continuous medium or solvent (η_s) (Rao, 1999):

$$\eta^{hs} = \eta_s(1 + 2.5\phi). \quad (10)$$

Combining Eqs. (9) and (10), the following expression is derived to estimate the contribution of colloidal forces to the relative viscosity, from viscosity data at different volume fractions:

$$\eta_r^{cf} = \frac{\eta^{cf}}{\eta_s} = \frac{\eta}{\eta_s} - (1 + 2.5\phi). \quad (11)$$

For diluted systems, Genovese and Lozano (2006b) proposed the following model to predict η_r^{cf} in terms of the normalized energy barrier and the volume fraction of particles:

$$\eta_r^{cf} = \alpha\left(\frac{U_{Max}}{k_BT}\right)\phi, \quad (12)$$

where α is a numerical constant.

3. Materials and methods

3.1. Sample preparation

Cloudy apple juice (cv. Granny Smith) was obtained from the juice factory Jugos S.A. (Río Negro, Argentina). Since the objective of this work was to study only the effect of liquid medium pH and I on the interaction and stability of juice particles, the first step was to remove the native pectins, sugars, organic acids, and inorganic salts from the juice. With this purpose, the juice was depectinized with a commercial pectolytic enzyme (Solvay 5XLHA; 20 mg/l, 2 h at 50 °C), the supernatant was separated from the degraded pectin sediment, and subjected to diafiltration in a lab-scale equipment Osmonic Sepa® CF (Osmonics, Minnetonka, MN, USA) with 100 kDa cutoff polysulfone membranes. The juice (700 ml) was diafiltered with distilled water until reaching pH = 4.5 and a conductivity equivalent to a 1×10^{-4} M KCl solution, determined from a calibration curve (Fig. 1).

The second step was to adjust the liquid medium pH and I with known amounts of acids and salts, respectively. Diafiltered juice was acidified through the addition of 1 N HCl solution (Anedra, Buenos Aires) until reaching values of pH = 3.1, 2.5 and 2.1. At the same time, the ionic strength of each sample was modified through the addition of KCl (Anedra, Buenos Aires), until reaching concentrations of [KCl] = 1×10^{-3}, 1×10^{-2} and 1×10^{-1} M. In this way, 16 different samples were obtained (4 pH × 4 [KCl]). Each sample was prepared in duplicate, using the same diafiltered juice. KCl was used to modify I because potassium (K^+) is the most abundant cation in apple juice (Eisele & Drake, 2005; Genovese & Lozano, 2006a; Van Buren, 1989). It should be noted that protons (H^+) arising from the dissociation of HCl in water are not free, but instead they form hydrogen bonds with water giving hydrated protons, also called hydronium cations (H_3O^+).

3.2. Particle size, ζ potential, and turbidity measurements

ζ potential (ζ), electric conductivity (C), and size distribution were measured at 25 °C in a Malvern Zetasizer

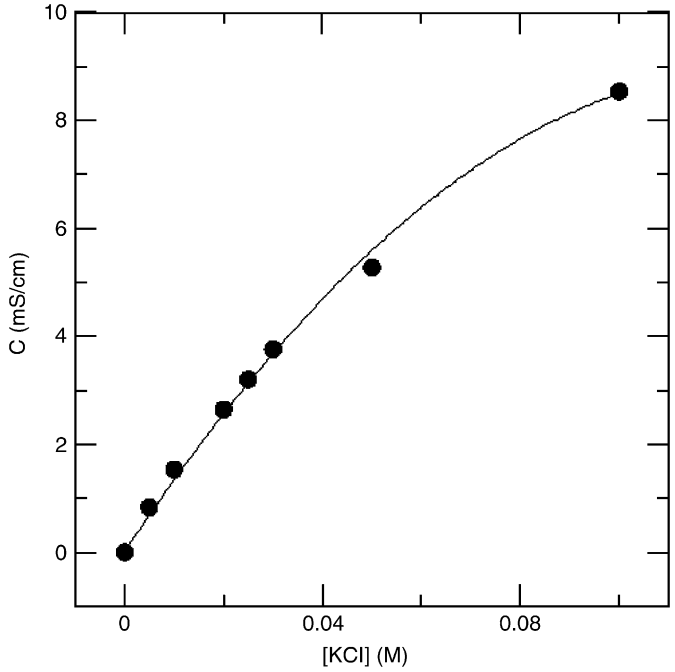

Fig. 1. Calibration curve of diafiltered juice electric conductivity as a function of KCl concentration.

3000 particle analyzer (Malvern Instrument Inc., London, UK). Each parameter was measured 10 times per sample.

Turbidity (τ) was measured at room temperature in a 15 ml standard vial using a PC Compact nephelometer (Aqualytic, Germany). Each sample was measured in duplicate, and allowed to settle for one hour in the vial before measurement.

3.3. Viscosity measurements

Kinematic viscosity ($v = \eta/\delta$) of six samples: $[KCl] = 1 \times 10^{-4}$ M—pHs 4.5 and 3.1, $[KCl] = 1 \times 10^{-2}$ M—pH 4.5, $[KCl] = 1 \times 10^{-1}$ M—pHs 4.5, 3.1 and 2.1, each one at different volume fractions, was measured at 25 °C in a Cannon-Fenske glass capillary viscometer (efflux times > 360 s), calibrated with distilled water (Liley, Thomson, Friend, Daubert, & Buck, 1999). Measurements were done in triplicate.

3.4. Particle volume fraction

Different particle volume fractions (ϕ) were obtained by diluting a suspension having a certain particle concentration, I and pH, with a solution having the same I and pH. In order to determine the particle volume fraction of the original suspension (ϕ_0), a 25 ml aliquot of diafiltered juice was lyophilized in a Heto FD 8.0 freeze dryer (Heto-Holten, Denmark). To initiate drying the heating plate temperature was set to 20 °C and the vacuum to 0.1 mBar. After drying for 48 h, apple juice particles were removed from trays and stored under vacuum in desiccators with P_2O_5 during 24 h. Particles weight was converted to volume using a particle density of $\delta_P = 1.2$ g/ml (cited in the review paper of Beveridge, 2002). Determination was done by duplicate.

4. Results and discussion

4.1. Parameters of the extended DLVO theory

In order to apply the extended DLVO theory (Eqs. (2), (3) and (6)), apple juice particles were considered to be approximately spherical (Genovese & Lozano, 2000, 2005b). An average hydrodynamic diameter was obtained from the particle size distribution of each sample. It was found that the average particle size did not change with medium conditions (pH and I). The resulting average particle radius was $a = 305 \pm 10$ nm.

The Hamaker constant involved in the calculation of Van der Waals energy (Eq. (2)) was estimated from Lifshitz theory (Israelachvili, 1992):

$$A = \frac{3}{4} k_B T \left(\frac{\varepsilon_p - \varepsilon}{\varepsilon_p + \varepsilon}\right)^2 + \frac{3h\nu_e}{16\sqrt{2}} \frac{(n_p^2 - n^2)^2}{(n_p^2 + n^2)^{3/2}}, \quad (13)$$

where sub-index "p" indicates particle, h is Planck's constant, ν_e is the main electronic absorption frequency in the UV, and n is the refractive index. Particle's properties were assumed to be independent of the liquid medium conditions, and approximately equal to the properties of pure protein: $\varepsilon_p = 4.43 \times 10^{-11}$ F/m, $n_p = 1.56$, and $\nu_e = 2.9 \times 10^{15}$ s^{-1} (Genovese & Lozano, 2006b; McClements, 1999). Considering the properties of the liquid medium (ε and n) approximately equal to those of water, the value $A = 3.86 k_B T$ was calculated with Eq. (13). This is a theoretically estimated value of the apple juice sol Hamaker constant, which should be experimentally confirmed in future works. However, it was considered to be a reasonable value when compared with those reported for other colloidal systems (see, for example, Chang & Chang, 2002; Yotsumoto & Yoon, 1993a, 1993b).

Debye's length (κ^{-1}) involved in the electrostatic repulsive energy (Eq. (3)) was calculated with Eq. (4) and reported in Table 3. As expected, κ^{-1} decreased at decreasing pH values (i.e. at increasing $[H_3O^+]$) and increasing [KCl], reflecting the compression of the electrical double layer at increasing I. In all cases, $\kappa^{-1} < a/10$, fulfilling the condition required for Eq. (3). Particle surface potential was determined indirectly through the measurement of ζ potential (ζ) (Chang & Chang, 2002; Overbeek, 1977). All the ζ values were negative in the range of pH and [KCl] studied (Fig. 2). The most negative ζ value was reached at the minimum H_3O^+ and KCl concentrations, i.e. pH = 4.5 and $[KCl] = 1 \times 10^{-4}$ M. Afterwards, ζ magnitudes decreased at increasing $[H_3O^+]$ and [KCl]. The effect of [KCl] on ζ was smaller at lower pH values. The individual and combined effects of pH and [KCl] on ζ were estimated by fitting the experimental data with the

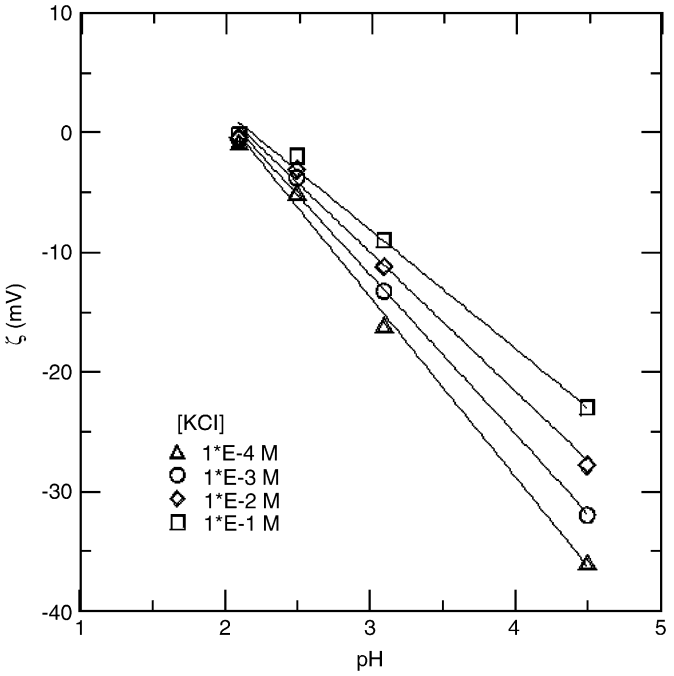

Fig. 2. Effect of pH on apple juice particles ζ potential at different KCl concentrations. Experimental values were fitted with Eq. (14).

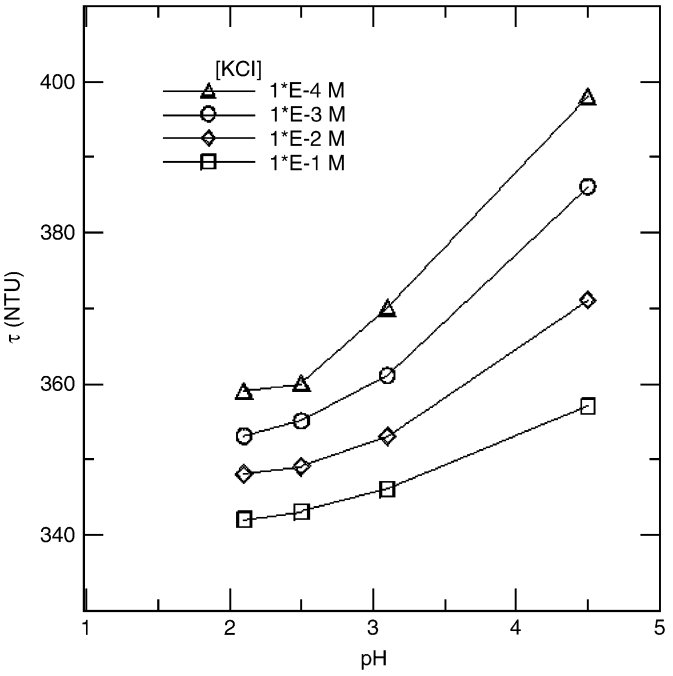

Fig. 3. Effect of pH on diafiltered juice turbidity, at different KCl concentrations.

following expression ($R^2 = 0.996$):

$$\zeta = 1.696\ \log([\mathrm{KCl}])\mathrm{pH} - 8.226\mathrm{pH} - 3.223\ \log([\mathrm{KCl}]) + 18.45, \quad (14)$$

which is valid in the range of pH and [KCl] studied. It can be visualized from Eq. (14) that although both HCl and KCl contributed to increase the medium I, their effects cannot be considered to be equivalent. On one hand, KCl contributed to reduce the electrical double layer surrounding the particles. On the other hand, H_3O^+ contributed to neutralize particles charge, reducing the attraction of counterions (K^+).

The decay length required for the calculation of the hydration energy (Eq. (6)) was considered to be approximately constant in the pH and I range studied in this work. Then, a unique value of $\lambda = 1$ nm was used as in the case of soy protein in water (Berli et al., 1999), and cloudy apple juice particles (Genovese & Lozano, 2006a, 2006b). Consequently, the only unknown parameter remaining in Eq. (6) was the hydration pressure constant (P_0), which is calculated later in this work.

4.2. Turbidity

Fig. 3 shows the variation of turbidity (τ) with pH and [KCl]. The highest τ value ($\approx$ 400 NTU) was obtained at the minimum H_3O^+ and KCl concentrations, i.e. pH = 4.5 and [KCl] = 1×10^{-4} M. Thereafter, τ values decreased at increasing [H_3O^+] and [KCl]. However, the minimum τ value ($\approx$ 340 NTU) was still relatively high. This suggests that although the electrostatic interaction was almost eliminated by reducing ζ values close to zero (Fig. 2), the particles remained stable.

As previously explained, turbidity is mainly a function of the energy barrier, and this one is governed by changes in ζ and P_0 values (as later demonstrated in this work). This effect was visualized by correlating turbidity and ζ potential for each [KCl] (Fig. 4). Experimental data were fitted with a quadratic polynomial:

$$\tau = \tau_H + b\zeta + c\zeta^2, \quad (15)$$

where τ_H could be considered as the contribution of hydration forces to turbidity (when $\zeta = 0$), and b and c are constants. Fitting parameters obtained for each [KCl] were listed in Table 1. Values of b and c did not show a clear trend with [KCl]. Furthermore, the common trend followed by all the four curves in Fig. 4 suggests that ζ had a unique effect on τ, which was shifted by [KCl]. This observation is confirmed next (Eqs. (16)–(18)).

The component τ_H followed a linear relationship with the logarithm of [KCl] (Fig. 5), according to the function ($R^2 = 0.999$):

$$\tau_H = -2.323\ln([\mathrm{KCl}]) + 337.0. \quad (16)$$

This means that the effect of hydrostatic forces on turbidity decreased at increasing [KCl]. Accepting that all the other terms in Eq. (6) remained constant, this result indicates that P_0 decreased at increasing I.

Considering that turbidity is maintained by repulsive forces, the last two terms in Eq. (15) may be considered as the contribution of electrostatic forces to turbidity (τ_E), such that Eq. (15) could be rewritten as

$$\tau = \tau_H + \tau_E. \quad (17)$$

The τ_E values obtained by difference from Eq. (17) were represented in Fig. 6, and analogously fitted with the

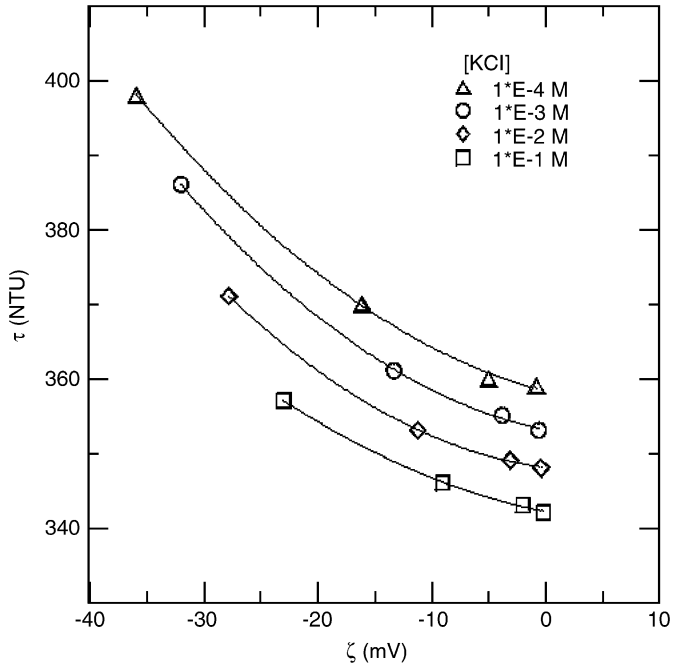

Fig. 4. Correlation between turbidity and ζ potential at different KCl concentrations.

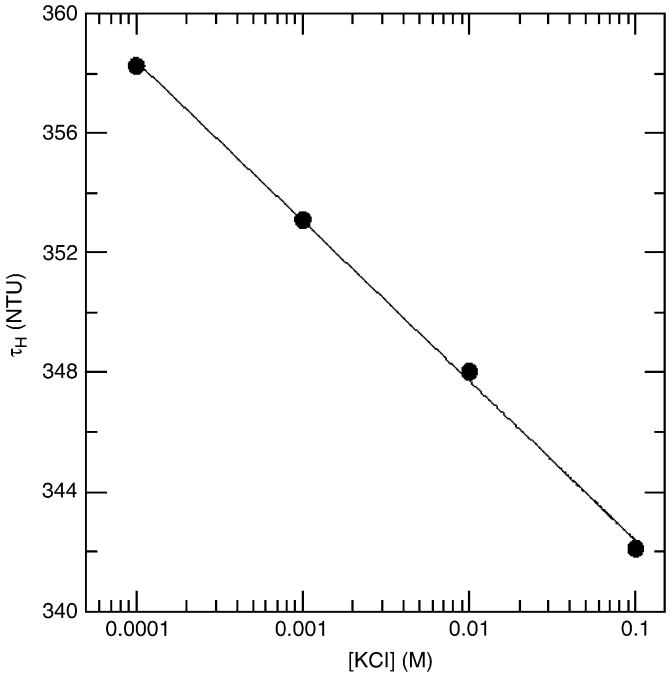

Fig. 5. Effect of KCl concentration on the turbidity component due to hydration forces.

Table 1
Eq. (15) fitting parameters for different [KCl]

[KCl] (M)	τ_H (NTU)	b (NTU/mV)	c (NTU/mV^2)	R^2
1.E−04	358.2	−0.390	0.020	0.9992
1.E−03	353.1	−0.307	0.022	0.9996
1.E−02	348.0	−0.195	0.023	0.9999
1.E−01	342.1	−0.308	0.015	0.9994

quadratic polynomial ($R^2 = 0.992$):

$$\tau_E = -0.197\zeta + 0.025\zeta^2. \quad (18)$$

The fact that a unique curve independent of [KCl] was obtained indicates that τ_E is basically governed by particles surface charge.

4.3. Viscosity—energy barrier correlation

Particle volume fraction of the diafiltered juice was determined to be $\phi_0 = 1.57 \times 10^{-3}$. Although the method employed to obtain ϕ_0 may suffer some inaccuracy because juice particles are likely to be highly hydrated, the value obtained here is of the same order of those determined for cloudy apple juice by other techniques (Genovese & Lozano, 2000, 2006b), and then it was considered to be satisfactory. Fig. 7 shows the contribution of colloidal forces to relative viscosity (η_r^{cf}) as a function of particle volume fraction (ϕ), at different conditions (pH-[KCl]) of the liquid medium. In all cases, data followed a linear trend as proposed by Genovese and Lozano (2006b) for diluted

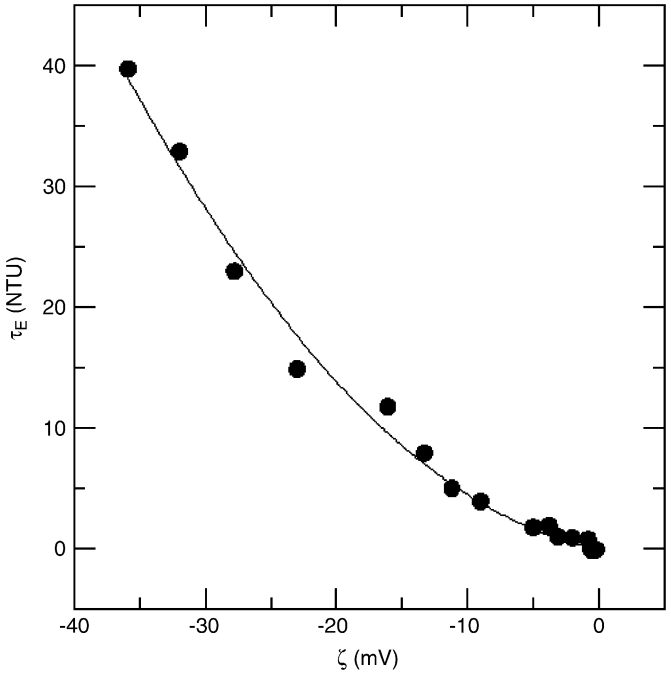

Fig. 6. Effect of ζ potential on the turbidity component due to electrostatic forces.

systems, and were fitted with Eq. (12). Resulting fitting parameters were listed in Table 2.

4.4. Turbidity—energy barrier correlation

It has been found in other colloidal suspensions that turbidity increases with increasing values of the energy

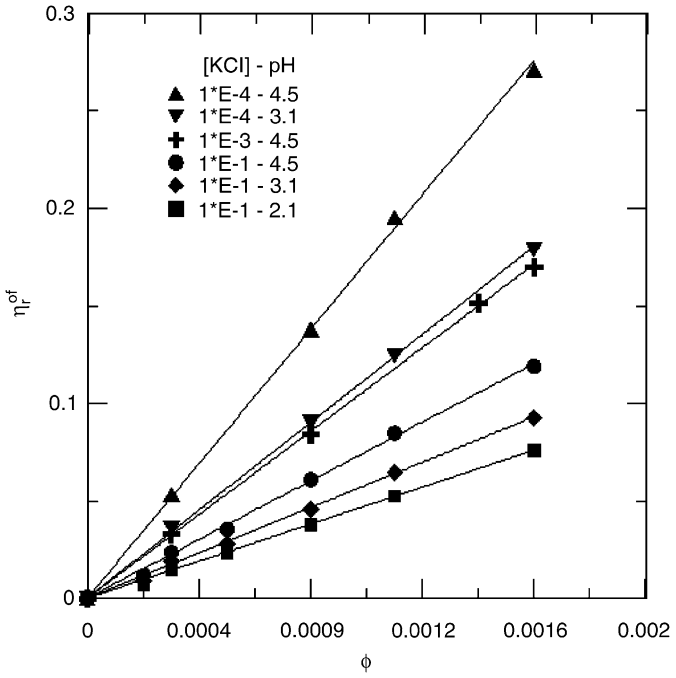

Fig. 7. Effect of particle volume fraction on the colloidal forces contribution to relative viscosity, for different liquid medium conditions.

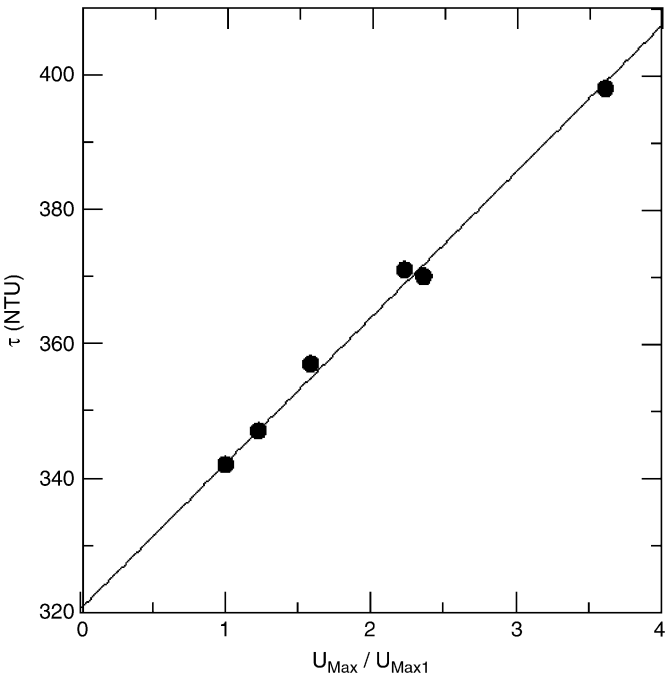

Fig. 8. Correlation between turbidity and energy barrier ratio.

Table 2
Eq. (12) fitting parameters for different pH-[KCl] conditions

pH	[KCl] (M)	α (U_{Max}/k_BT)	R^2
4.5	1.E−04	174.0	0.9995
3.1	1.E−04	113.7	0.9996
4.5	1.E−02	107.4	0.9999
4.5	1.E−01	76.22	0.9997
3.1	1.E−01	58.88	0.9998
2.1	1.E−01	48.08	0.9990

barrier (Chang & Chang, 2002), until a maximum is reached (Yotsumoto & Yoon, 1993a, 1993b). However, the turbidity-energy barrier relationship was not modeled in those works. The following procedure was used in this study. First, the sample with both lowest τ and lowest $\alpha(U_{Max}/k_BT)$ value in Table 2, i.e. [KCl] $= 1 \times 10^{-1}$ M and pH $= 2.1$, was selected as the reference sample and identified with sub-index "1". Considering α (Eq. (12)) to be the same for all samples, the energy barrier ratios between each sample and the reference sample were obtained from Table 2. It was found that the turbidity of these samples was directly proportional to the energy barrier ratio (Fig. 8). Then, experimental data were fitted with the expression

$$\tau = \frac{U_{Max}}{U_{Max,1}}(\tau_1 - \tau_0) + \tau_0, \tag{19}$$

where τ_0 is the unique fitting parameter in Eq. (19), and represents the turbidity at $U_{Max} = 0$. The value obtained was $\tau_0 = 320.3$ NTU, with $R^2 = 0.994$. The regression coefficient was highly satisfactory, indicating that the turbidity of an apple juice sol follows a linear relationship with the energy barrier in the pH and I ranges studied in this work. Then, Eq. (19) may be conveniently rewritten in the general form as

$$\tau = \tau_0 + \beta \frac{U_{Max}}{k_BT}, \tag{20}$$

where β is a constant independent of medium conditions ([KCl] and pH). Eqs. (19) and (20) might be applicable to other colloidal suspensions in a certain energy barrier range, which should be confirmed experimentally for each system. As previously mentioned, the value of τ_0 represents the sol turbidity when there is no net repulsive energy between particles. Consequently, the high τ_0 value obtained indicates that particles are inherently stable. One possible explanation is that they are strongly hydrated by an immobilized water layer coating them (the primary hydration shell). Consequently, changes in pH and I would affect the stability parameters starting from the secondary hydration shell.

4.5. Energy barrier and hydration constant determination

The first step to determine the individual U_{Max} values was to calculate the ratio between the two highest U_{Max} values, which were obtained at [KCl] $= 1 \times 10^{-4}$ M and pH $= 4.5$ and 3.1, respectively. Those samples were chosen because it was assumed that the difference between their U_{Max} values might be attributed mainly to changes in U_E,

and that the effect of I changes by acidification on U_H was negligible. The calculated ratio was:

$$\frac{U_{Max(\mathrm{pH}=4.5)}}{U_{Max(\mathrm{pH}=3.1)}} = 1.530. \quad (21)$$

The simultaneous resolution of Eq. (21) with Eqs. (7) and (8) required an extra condition. Then it was assumed that $X(\mathrm{pH}\ 4.5) = X(\mathrm{pH}\ 3.1)$. This supposition was based on an empirical observation: Eq. (21) was fulfilled when X values for both energy barriers were very similar and close to 0.4 nm. The solution of the equation system gave values of $P_0\,(\mathrm{pH}\ 4.5) = 12.40\,\mathrm{mJ/m^2}$ and $P_0\,(\mathrm{pH}\ 3.1) = 12.48\,\mathrm{mJ/m^2}$. These values were used to calculate the corresponding energy barriers: $U_{Max}\,(\mathrm{pH}\ 4.5) = 652.3\,k_BT$ and $U_{Max}\,(\mathrm{pH}\ 3.1) = 426.3k_BT$. These results were applied into Eq. (12) to calculate the values of $\alpha = 0.2667$, and U_{Max} of the other four samples represented in Fig. 7. Correlating the U_{Max} values of these six samples with their corresponding turbidities, the values of $\beta = 0.1205$ NTU, and the energy barriers of the other ten samples were obtained from Eq. (19). These U_{Max} values were used to calculate the P_0 and X values of all the remaining samples (Table 3).

In general, P_0 decreased at increasing $[H_3O^+]$ and [KCl]. Similar trends were found in other systems (Chang & Chang, 2002; Yotsumoto & Yoon, 1993b), and may be explained as follows. As previously proposed, hydrogen bonding between the hydrogen of the –OH groups of polysaccharide molecules and the oxygen of water molecules created a primary hydration shell coating the particle, followed by a secondary (weaker) hydration shell, and so on. It seems that H_3O^+ and hydrated K^+ cations attracted by particle's negative charge, approached particle's environs and distorted the outer hydration shells, reducing the hydration force. This suggests that the repulsive hydration force is an inherent property of apple juice particles, rather than a secondary effect created by the adsorption of hydrated cations. Finally, it should be noted that K^+ cations produced more distortion than H_3O^+ cations, probably due to the bigger size of the formers (Israelachvili, 1992).

Calculated U_{Max} values followed the same trend as P_0 and ζ magnitudes, respectively, i.e. decreased at increasing $[H_3O^+]$ and [KCl], confirming that U_{Max} was governed by the changes in P_0 and ζ. Calculated X values ranged from 0.40 to 0.51 nm, fulfilling the condition $X \ll a$ required for

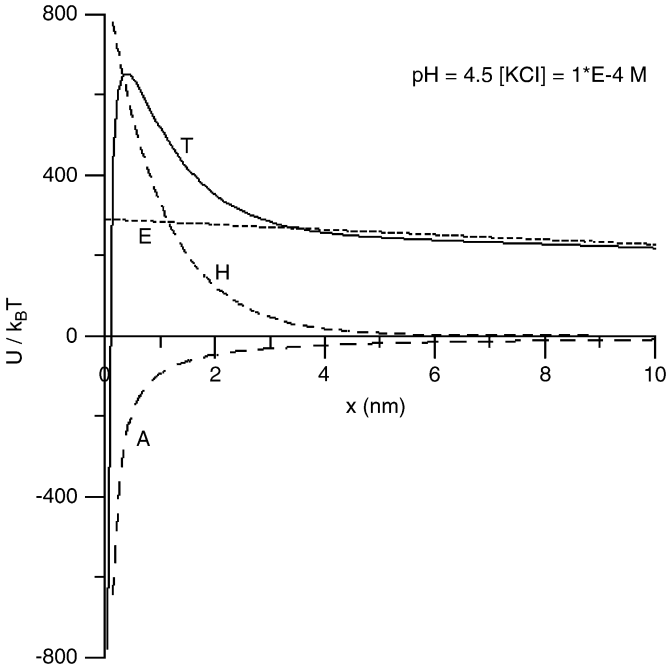

Fig. 9. Hydration (H), Electrostatic (E), Van der Waals (A), and total (T) interaction energies (normalized with Brownian thermal energy) as a function of interparticle distance, for the diafiltered juice.

Table 3
Values of hydration constant (P_0), energy barrier (U_{Max}), interparticle distance where U_{Max} is located (X), and Debye's length (κ^{-1}) at different pH-[KCl] conditions

	[KCl] (M)	1.E−04	1.E−03	1.E−02	1.E−01
pH = 4.5	P_0 (mJ/m^2)	12.40	11.51	9.90	8.96
	U_{Max} (k_BT)	652.3	545.5	402.4	286.1
	X (nm)	0.40	0.41	0.44	0.45
	κ^{-1} (nm)	30.70	9.71	3.07	0.97
pH = 3.1	P_0 (mJ/m^2)	12.48	11.04	9.90	9.08
	U_{Max} (k_BT)	426.3	337.8	271.4	221.4
	X (nm)	0.40	0.43	0.46	0.48
	κ^{-1} (nm)	10.86	7.24	2.95	0.97
pH = 2.5	P_0 (mJ/m^2)	11.56	10.73	9.68	8.61
	U_{Max} (k_BT)	329.5	288.0	238.2	188.3
	X (nm)	0.42	0.44	0.47	0.50
	κ^{-1} (nm)	5.51	4.79	2.68	0.96
pH = 2.1	P_0 (mJ/m^2)	11.49	10.44	9.54	8.44
	U_{Max} (k_BT)	321.2	271.4	229.9	180.7
	X (nm)	0.42	0.44	0.47	0.51
	κ^{-1} (nm)	3.48	3.27	2.30	0.94

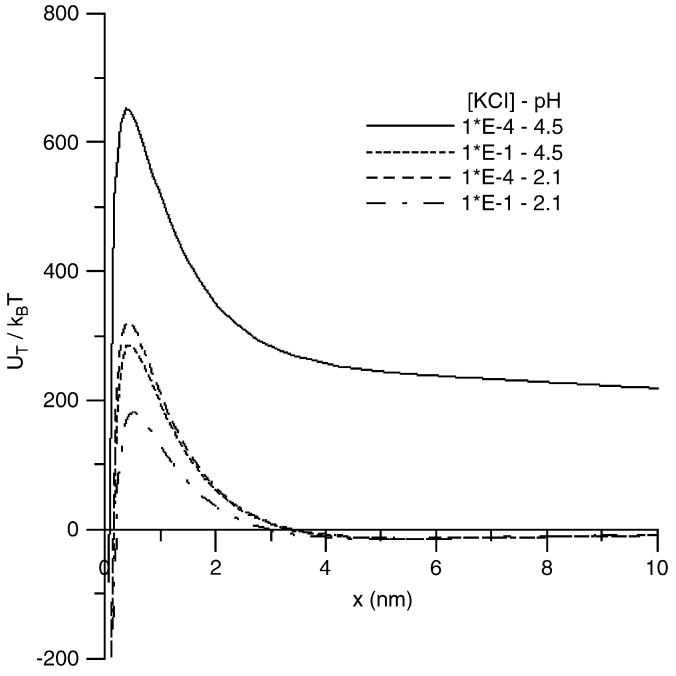

Fig. 10. Total interaction energy (normalized with Brownian thermal energy) as a function of interparticle distance, for different liquid medium conditions.

Eq. (2). Fig. 9 shows the hydration, electrostatic, Van der Waals, and total interaction energies between particles of the diafiltered juice, calculated with Eqs. (6), (3), (2), and (7), respectively. As expected, at close separations the short-range hydration forces were higher than electrostatic forces, indicating that hydration was the main contribution to particle stability, as found in other systems (Berli et al., 1999; Genovese & Lozano, 2006b). Fig. 10 shows the total interaction energy curves of four representative samples: pH = 4.5—[KCl] = 1×10^{-4} and 1×10^{-1} M, and pH = 2.1—[KCl] = 1×10^{-4} and 1×10^{-1} M, obtained from Eq. (7).

5. Conclusions

The extended DLVO theory appropriately explained the stability of colloidal apple juice particles from turbidity and viscosity data. It was possible to predict the individual contribution of repulsive electrostatic and hydration forces to sol turbidity, respectively. Reducing the pH and increasing I of the liquid medium reduced the energy barrier between apple juice particles, due to the reduction of both their hydration constant and their ζ potential magnitudes. The decrease of the energy barrier produced a linear decrease in the sol turbidity. However, the turbidity remained high even with no energy barrier indicating that apple juice particles are inherently stable, phenomena attributed to the primary hydration shell coating them. The reduction of the hydration constant was attributed to the distortion of the outer hydration shells by H_3O^+ and hydrated K^+ cations, attracted by negative charged particles.

Acknowledgements

This research was supported by a grant (PICT No. 09-08016) from the Agencia Nacional de Promoción Científica y Tecnológica of Argentina.

References

Berli, C. L. A., Deiber, J. A., & Añón, M. C. (1999). Connection between rheological parameters and colloidal interactions of a soy protein suspension. *Food Hydrocolloids*, *13*, 507–515.

Besseling, N. A. M. (1997). Theory of hydration forces between surfaces. *Langmuir*, *13*(7), 2113–2122.

Beveridge, T. (2002). Opalescent and cloudy fruit juices: Formation and particle stability. *Critical Reviews in Food Science and Nutrition*, *42*(4), 317–337.

Bostrom, M., Williams, D. R. M., & Ninham, B. W. (2001). Specific ion effects in colloid interactions: Why DLVO theory fails for biology. *Physical Review Letters*, *87*(16), 1–4.

Brillouet, J. M., Williams, P., Will, F., Müller, G., & Pellerin, P. (1996). Structural characterization of apple juice arabinogalactan-protein which aggregates following enzymic dearabinosylation. *Carbohydrate Polymers*, *29*, 271–275.

Chang, Y. I., & Chang, P. K. (2002). The role of hydration force on the stability of the suspension of *Saccharomyces cerevisiae*. Application of the extended DLVO theory. *Colloids and Surfaces A*, *211*, 67–77.

Derjaguin, B. V. (1989). *Theory of stability of colloids and thin films*. New York: Consultant Bureau Ed.

Dietrich, H., Gierschner, K., Pecoroni, S., Zimmer, E., & Will, F. (1996). New findings regarding the phenomenon of cloud stability. *Flussiges Obst*, *63*(1), 7–10.

Eisele, T. A., & Drake, S. R. (2005). The partial compositional characteristics of apple juice from 175 apple varieties. *Journal of Food Composition and Analysis*, *18*(2–3), 213–221.

Genovese, D. B., & Lozano, J. E. (2000). Effect of cloud particle characteristics on the viscosity of cloudy apple juice. *Journal of Food Science*, *65*(4), 641–645.

Genovese, D. B., & Lozano, J. E. (2006a). Stability of cloudy apple juice colloidal particles modeled with the extended DLVO theory. In P. Bruera, J. Welti-Chanes, P. Lillford, & H. Corti (Eds.), *Water properties of food, pharmaceutical, and biological materials*. Boca Raton, FL: CRC Press pp. 289–300.

Genovese, D. B., & Lozano, J. E. (2006b). Contribution of colloidal forces to the viscosity and stability of cloudy apple juice. *Food Hydrocolloids* (in press).

Grasso, D., Subramaniam, K., Butkus, M., Strevett, K., & Bergendahl, J. (2002). A review of non-DLVO interactions in environmental colloidal systems. *Environmental Science and Biotechnology*, *1*, 17–38.

Israelachvili, J. N. (1992). *Intermolecular and surface forces*. New York: Academic Press.

Liley, P. E., Thomson, G. H., Friend, D. G., Daubert, T. E., & Buck, E. (1999). Physical & chemical data. In R. H. Perry, D. W. Green, & J. O. Maloney (Eds.), *Perry's chemical engineers' handbook* (7th ed). New York: McGraw-Hill Companies.

Magdassi, S., & Kamyshny, A. (1996). Surface activity and functional properties of proteins. In S. Magdassi (Ed.), *Surface activity of proteins: Chemical and physicochemical modifications*. New York: Marcel Dekker.

McClements, D. J. (1999). *Food emulsions: Principles, practice, and techniques*. Boca Raton, FL: CRC Press.

Ogawa, A., Yamada, H., Matsuda, S., & Okajima, K. (1997). Viscosity equation for concentrated suspensions of charged colloidal particles. *Journal of Rheology*, *41*(3), 769–785.

Overbeek, J. Th. G. (1977). Recent developments in the understanding of colloid stability. In M. Kerker, A. C. Zettlemoyer, & R. L. Rowell (Eds.), *Colloid and interface science* (pp. 431–445). New York: Academic Press.

Quemada, D., & Berli, C. (2002). Energy of interaction in colloids and its implications in rheological modeling. *Advances in Colloid and Interface Science*, *98*, 51–85.

Rao, M. A. (1999). *Rheology of fluid and semisolid foods: Principles and applications*. Gaithersburg, MD: Aspen Publishers.

Sennet, P., & Olivier, J. P. (1965). Colloidal dispersions, electrokinetic effects and the concept of zeta potential. In D. E. Gushee (Ed.), *Chemistry and physics of interfaces* (pp. 74–92). Washington, DC: American Chemical Society Publications.

Sorrivas, V., Genovese, D. B., & Lozano, J. E. (2006). Micrographic study of the effect of pectinolytic and amylolitic enzymes on apple juice turbidity. *Journal of Food Processing and Preservation*, *30*(2).

Van Buren, J. P. (1989). Causes and prevention of turbidity in apple juice. In D. L. Downing (Ed.), *Processed apple products* (pp. 97–120). New York: Van Nostrand Reinhold.

Yamasaki, M., Yasui, T., & Arima, K. (1964). Pectic enzymes in the clarification of apple juice. *Agricultural and Biological Chemistry*, *28*(11), 779–787.

Yotsumoto, H., & Yoon, R. H. (1993a). Application of extended DLVO theory: Stability of rutile suspensions. *Journal of Colloid and Interface Science*, *157*, 426–433.

Yotsumoto, H., & Yoon, R. H. (1993b). Application of extended DLVO theory: Stability of silica suspensions. *Journal of Colloid and Interface Science*, *157*, 434–441.

Zavitsas, A. A. (2001). Properties of water solutions of electrolytes and nonelectrolytes. *Journal of Physical Chemistry B*, *105*, 7805–7815.